Real-time assessment of renal cortical microvascular perfusion heterogeneities using near-infrared laser speckle imaging

Rick Bezemer,[1,2,5]* Matthieu Legrand,[1,3,5] Eva Klijn,[2] Michal Heger,[4] Ivo C. J. H. Post,[4] Thomas M. van Gulik,[4] Didier Payen,[3] and Can Ince[1,2]

[1]*Department of Translational Physiology, Academic Medical Center, University of Amsterdam, Amsterdam, The Netherlands.*
[2]*Department of Intensive Care, Erasmus Medical Center, Erasmus University Rotterdam, Rotterdam, The Netherlands*
[3]*Department of Anesthesiology and Critical Care, Lariboisière Hospital, Assistance Publique-Hopitaux de Paris, University of Paris, Paris, France.*
[4]*Department of Experimental Surgery, Academic Medical Center, University of Amsterdam, Amsterdam, The Netherlands*
[5]*These authors contributed equally to this work.*
*R.Bezemer@amc.uva.nl

Abstract: Laser speckle imaging (LSI) is able to provide full-field perfusion maps of the renal cortex and allows quantification of the average LSI perfusion within an arbitrarily set region of interest and the recovery of LSI perfusion histograms within this region. The aim of the present study was to evaluate the use of LSI for mapping renal cortical microvascular perfusion and to demonstrate the capability of LSI to assess renal perfusion heterogeneities. The main findings were that: 1) full-field LSI measurements of renal microvascular perfusion were highly correlated to single-point LDV measurements; 2) LSI is able to detect differences in reperfusion dynamics following different durations of ischemia; and 3) renal microvascular perfusion heterogeneities can be quantitatively assessed by recovering LSI perfusion histograms.

©2010 Optical Society of America

OCIS codes: (0110) Imaging systems; (0170) Medical optics and biotechnology

References and links

1. N. Lameire, W. Van Biesen, and R. Vanholder, "Acute renal failure," Lancet **365**(9457), 417–430 (2005).
2. A. J. McLaren, W. Jassem, D. W. Gray, S. V. Fuggle, K. I. Welsh, and P. J. Morris, "Delayed graft function: risk factors and the relative effects of early function and acute rejection on long-term survival in cadaveric renal transplantation," Clin. Transplant. **13**(3), 266–272 (1999).
3. S. I. Myers, L. Wang, F. Liu, and L. L. Bartula, "Suprarenal aortic clamping and reperfusion decreases medullary and cortical blood flow by decreased endogenous renal nitric oxide and PGE2 synthesis," J. Vasc. Surg. **42**(3), 524–531 (2005).
4. M. Legrand, E. G. Mik, T. Johannes, D. Payen, and C. Ince, "Renal hypoxia and dysoxia after reperfusion of the ischemic kidney," Mol. Med. **14**(7-8), 502–516 (2008).
5. M. Legrand, E. Almac, E. G. Mik, T. Johannes, A. Kandil, R. Bezemer, D. Payen, and C. Ince, "L-NIL prevents renal microvascular hypoxia and increase of renal oxygen consumption after ischemia-reperfusion in rats," Am. J. Physiol. Renal Physiol. **296**(5), F1109–F1117 (2009).
6. L. Wu, M. M. Tiwari, K. J. Messer, J. H. Holthoff, N. Gokden, R. W. Brock, and P. R. Mayeux, "Peritubular capillary dysfunction and renal tubular epithelial cell stress following lipopolysaccharide administration in mice," Am. J. Physiol. Renal Physiol. **292**(1), F261–F268 (2006).
7. T. Yamamoto, T. Tada, S. V. Brodsky, H. Tanaka, E. Noiri, F. Kajiya, and M. S. Goligorsky, "Intravital videomicroscopy of peritubular capillaries in renal ischemia," Am. J. Physiol. Renal Physiol. **282**(6), F1150–F1155 (2002).
8. J. V. Bonventre, and J. M. Weinberg, "Recent advances in the pathophysiology of ischemic acute renal failure," J. Am. Soc. Nephrol. **14**(8), 2199–2210 (2003).
9. R. Bellomo, C. Ronco, J. A. Kellum, R. L. Mehta, P. Palevsky, "Acute renal failure - definition, outcome measures, animal models, fluid therapy and information technology needs: the Second International Consensus Conference of the Acute Dialysis Quality Initiative (ADQI) Group," Crit. Care **8**(4), R204–R212 (2004).

#125295 - $15.00 USD Received 11 Mar 2010; revised 6 May 2010; accepted 12 May 2010; published 30 Jun 2010

10. P. M. O'Connor, "Renal oxygen delivery: matching delivery to metabolic demand," Clin. Exp. Pharmacol. Physiol. **33**(10), 961–967 (2006).
11. C. Rosenberger, S. Rosen, and S. N. Heyman, "Renal parenchymal oxygenation and hypoxia adaptation in acute kidney injury," Clin. Exp. Pharmacol. Physiol. **33**(10), 980–988 (2006).
12. J. O'Doherty, P. McNamara, N. T. Clancy, J. G. Enfield, and M. J. Leahy, "Comparison of instruments for investigation of microcirculatory blood flow and red blood cell concentration," J. Biomed. Opt. **14**(3), 034025 (2009).
13. A. M. Gorbach, H. Wang, N. N. Dhanani, F. A. Gage, P. A. Pinto, P. D. Smith, A. D. Kirk, and E. A. Elster, "Assessment of critical renal ischemia with real-time infrared imaging," J. Surg. Res. **149**(2), 310–318 (2008).
14. J. M. Coremans, M. Van Aken, D. C. Naus, M. L. Van Velthuysen, H. A. Bruining, and G. J. Puppels, "Pretransplantation assessment of renal viability with NADH fluorimetry," Kidney Int. **57**(2), 671–683 (2000).
15. J. T. Fitzgerald, S. Demos, A. Michalopoulou, J. L. Pierce, and C. Troppmann, "Assessment of renal ischemia by optical spectroscopy," J. Surg. Res. **122**(1), 21–28 (2004).
16. R. N. Raman, C. D. Pivetti, D. L. Matthews, C. Troppmann, and S. G. Demos, "A non-contact method and instrumentation to monitor renal ischemia and reperfusion with optical spectroscopy," Opt. Express **17**(2), 894–905 (2009).
17. R. Bezemer, E. Klijn, M. Khalilzada, A. Lima, M. Heger, J. van Bommel, and C. Ince, "Validation of near-infrared laser speckle imaging for assessing microvascular (re)perfusion," Microvasc. Res. **79**(2), 139–143 (2010).
18. J. D. Briers, "Laser Doppler, speckle and related techniques for blood perfusion mapping and imaging," Physiol. Meas. **22**(4), R01–R66 (2001).
19. Z. Wang, S. Hughes, S. Dayasundara, and R. S. Menon, "Theoretical and experimental optimization of laser speckle contrast imaging for high specificity to brain microcirculation," J. Cereb. Blood Flow Metab. **27**(2), 258–269 (2007).
20. H. Cheng, Q. Luo, Z. Wang, H. Gong, S. Chen, W. Liang, and S. Zeng, "Efficient characterization of regional mesenteric blood flow by use of laser speckle imaging," Appl. Opt. **42**(28), 5759–5764 (2003).
21. B. Choi, N. M. Kang, and J. S. Nelson, "Laser speckle imaging for monitoring blood flow dynamics in the in vivo rodent dorsal skin fold model," Microvasc. Res. **68**(2), 143–146 (2004).
22. B. Walter, R. Bauer, A. Krug, T. Derfuss, F. Traichel, and N. Sommer, "Simultaneous measurement of local cortical blood flow and tissue oxygen saturation by Near infra-red Laser Doppler flowmetry and remission spectroscopy in the pig brain," Acta Neurochir. Suppl. (Wien) **81**, 197–199 (2002).
23. A. K. Dunn, H. Bolay, M. A. Moskowitz, and D. A. Boas, "Dynamic imaging of cerebral blood flow using laser speckle," J. Cereb. Blood Flow Metab. **21**(3), 195–201 (2001).
24. K. R. Forrester, C. Stewart, J. Tulip, C. Leonard, and R. C. Bray, "Comparison of laser speckle and laser Doppler perfusion imaging: measurement in human skin and rabbit articular tissue," Med. Biol. Eng. Comput. **40**(6), 687–697 (2002).
25. C. J. Stewart, R. Frank, K. R. Forrester, J. Tulip, R. Lindsay, and R. C. Bray, "A comparison of two laser-based methods for determination of burn scar perfusion: laser Doppler versus laser speckle imaging," Burns **31**(6), 744–752 (2005).
26. A. Gorbach, D. Simonton, D. A. Hale, S. J. Swanson, and A. D. Kirk, "Objective, real-time, intraoperative assessment of renal perfusion using infrared imaging," Am. J. Transplant. **3**(8), 988–993 (2003).
27. T. Johannes, E. G. Mik, and C. Ince, "Nonresuscitated endotoxemia induces microcirculatory hypoxic areas in the renal cortex in the rat," Shock **31**(1), 97–103 (2009).
28. T. Johannes, E. G. Mik, K. Klingel, H. J. Dieterich, K. E. Unertl, and C. Ince, "Low-dose dexamethasone-supplemented fluid resuscitation reverses endotoxin-induced acute renal failure and prevents cortical microvascular hypoxia," Shock **31**(5), 521–528 (2009).

1. Introduction

Ischemia/reperfusion (I/R) injury is a leading cause of acute kidney injury (AKI) and occurs during various conditions in surgical and critically ill patients [1–3]. The pathophysiology of I/R-induced AKI involves a complex interplay between renal hemodynamics, tubular injury, and inflammatory processes. Several experimental studies have shown that I/R-induced microcirculatory dysfunction is a central player in the development of AKI, depressing tissue perfusion and oxygenation [e.g., 4,5]. Various studies using direct observation of the tubular capillaries as well as direct observation of glomerular microcirculation have shown microcirculatory obstruction precedes renal dysfunction [6,7]. I/R-induced renal microvascular and parenchymal disorders are distributed heterogeneously within the kidney and develop in time [8]. A major contributing factor to the lack of significant progress in the prevention and management of AKI has been attributed to the lack of insight into the pathophysiological mechanisms underlying the progress to AKI due to the unavailability of suitable technologies for studying the heterogeneous nature of renal microvascular perfusion disorders [9–11].

#125295 - $15.00 USD Received 11 Mar 2010; revised 6 May 2010; accepted 12 May 2010; published 30 Jun 2010
(C) 2010 OSA

Several techniques can be used for the assessment of the renal cortical microvascular perfusion heterogeneities, e.g., scanning laser Doppler velocimetry (LDV) [12], thermography or infrared imaging [13], and nicotinamide adenine dinucleotide dehydrogenase (NADH) autofluorescence imaging [14–16]. However, each of these measurement techniques has specific shortcomings that limit their ability to map renal cortical perfusion heterogeneities, as discussed in more detail in the Discussion and conclusions section. A technique potentially overcoming these shortcomings is laser speckle imaging (LSI) [17–19]. The main advantage of LSI with respect to clinical and experimental applicability is the capability to directly measure tissue perfusion in large areas (e.g., complete organ surfaces) in a non-contact manner at high spatial and temporal resolution using a simple setup including a laser diode for illumination and a grayscale CCD camera. An additional advantage of using a conventional CCD camera is that it allows a normal video mode for identification of organ surfaces, complementing the quantitative LSI data with anatomical and morphological detail.

LSI provides full-field perfusion maps of the renal cortex and allows quantification of the average LSI perfusion within an arbitrarily set region of interest and the recovery of LSI perfusion histograms within this region. The aim of the present study was to evaluate the use of LSI for mapping renal cortical microvascular perfusion and to demonstrate the capability of LSI to assess renal perfusion heterogeneities. For this purpose, LSI was employed in two models of renal I/R experiments: 1) complete renal I/R and 2) heterogeneous renal I/R. In addition, complete renal I/R experiments were performed with 1, 10, and 45 min of ischemia to show differences in reperfusion dynamics following different durations of ischemia. In the 1 min complete renal I/R experiments, moreover, linear regression and correlation analysis was performed on full-field LSI measurements of renal microvascular perfusion versus single-point LDV measurements.

2. Materials and methods

2.1 Animal preparation

Twenty male Wistar rats (311-348 g) were used for this study. The animal protocol was approved by the animal ethics committee of the Academic Medical Center at the University of Amsterdam. Animal care and handling were performed in accordance with the guidelines for institutional and animal care and use committees.

The rats were anesthetized with an intraperitoneal injection of 90 mg/kg ketamine, 0.25 mg/kg medetomidine, and 0.05 mg/kg atropine-sulfate. Ketamine (50 mg/kg/h) was infused intravenously to maintain anesthesia. The animals were mechanically ventilated with a fraction of inspired oxygen of 0.4. Body temperature was maintained at 37 ± 0.5°C by external warming. The ventilator settings were adjusted to maintain an arterial partial pressure of CO_2 between 35 and 40 mmHg. A catheter was placed in the right carotid artery to monitor systolic and diastolic arterial blood pressure (SBP and DBP [mmHg], respectively) and heart rate. Mean arterial blood pressure (MAP [mmHg]) was calculated as MAP = DBP + (SBP-DBP)/3. The right jugular vein was cannulated for continuous infusion of Ringer's lactate. The left kidney was exposed via an incision of the left flank and immobilized in a Lucite kidney cup (K. Effenberger, Pfaffingen, Germany). A perivascular ultrasonic transient time flow probe (Transonic Systems, Ithaca, NY) was placed around the left renal artery and connected to a flow meter (model T206, Transonic Systems) for continuous measurement of renal blood flow (RBF [ml/min]).

2.2 Renal I/R experiments

Two types of renal I/R experiments were performed: complete I/R (n = 15) and heterogeneous I/R (n = 5). Complete renal I/R was achieved by suprarenal aortic occlusion, where the durations of the ischemic episodes were 1 min (n = 5), 10 min (n = 5), and 45 min (n = 5). In the 1 min I/R experiments, LSI was performed in combination with LDV and in the 10 and 45 min I/R experiments, only LSI was performed. As a heterogeneous model of renal I/R, air

#125295 - $15.00 USD Received 11 Mar 2010; revised 6 May 2010; accepted 12 May 2010; published 30 Jun 2010
(C) 2010 OSA

bubble-enriched isotonic saline was infused via a catheter in the right carotid artery (n = 5), resulting in a random obstruction of microcirculatory branches.

2.3 Laser speckle imaging

LSI is based on the formation of an interference pattern (or speckle pattern) on a CCD camera when a diffuse surface (e.g., biological tissue) is illuminated with highly coherent light such as that from a laser or laser diode [17–21]. Movement of scattering particles (e.g., red blood cells within the illuminated tissue volume) will influence the speckle pattern in time. Hence, tissue perfusion in the field of view results in fluctuations in a dynamic speckle pattern. By integrating these fluctuations over the CCD camera exposure time (typically ~4 ms), pixel areas with a high level of perfusion will have lower contrast whereas pixel areas with a low level of perfusion will have higher contrast. The optimal exposure time for the LSI system depends on the red blood cell velocities; for measuring high velocities, rapidly blurring the speckle image, short exposure times are required and for the detection of low velocities, longer exposure times are required. The speckle contrast, defined as the ratio of the standard deviation to the mean grayscale intensity in a small pixel window (i.e., 5 × 5 pixels), is related to the average velocity of the moving particles, which is expressed in flux as described elsewhere [18–21].

2.4 Laser speckle imaging setup

For LSI measurements, a commercially available system was used (Moor Instruments, Devon, UK). A 785-nm class 1 laser diode was employed for illumination of the tissue to a depth of approximately 1 mm. Directly reflected light by the tissue surface was blocked by a tunable polarization filter placed in front of the lens system since it was not scattered by flowing red blood cells and therefore contained no information on tissue perfusion. Laser speckle images were acquired using a 576 × 768 pixels grayscale CCD camera at a frame rate of 25 Hz and converted to pseudo-color images where the contrast (thus the level of perfusion) was scaled from blue (low perfusion) to red (high perfusion). The lens system allowed a variable zoom, ranging from 0.6 × 0.8 cm (corresponding to 10 µm/pixel) to 9 × 12 cm at a working distance of 15-45 cm, and focus optimization. For LSI of the rat kidney, the field of view was set to ~1.8 × 2.4 cm (corresponding to ~30 µm/pixel). Using a 5 × 5 pixel window to calculate speckle contrast, the maximal image resolution was ~150 µm/pixel area.

2.5 Laser speckle image analysis

LSI provides full-field perfusion maps of the renal cortex and allows quantification of the average LSI perfusion within an arbitrarily set region of interest and the recovery of LSI perfusion histograms within this region. For the complete renal I/R experiments, the average LSI perfusion value was determined per image (25 images/s) for the entire renal cortex in the field of view. For the heterogeneous renal I/R experiments, LSI perfusion histograms were recovered from each image (25 images/s) for the entire renal cortex in the field of view. The histograms were fitted with a Gaussian fit and analyzed for mean ± SD LSI perfusion. The SD of the Gaussian fit of the LSI perfusion histograms was interpreted as a measure of perfusion heterogeneity.

2.6 Laser Doppler velocimetry setup

LDV was performed using the O2C system (Oxygen to See; LEA Medizintechnik, Giessen, Germany). Since the LDV device employs a similar light source (i.e., 785-nm class 1 laser diode) as the LSI device, measurement depth within the kidney was approximately equal for both techniques (i.e., limited to the renal cortex). LDV-measured perfusion was expressed as flux, similarly to the LSI-measured perfusion. The LDV system has been validated by comparison to perfusion measurements using colored microspheres in the pig brain [22].

#125295 - $15.00 USD Received 11 Mar 2010; revised 6 May 2010; accepted 12 May 2010; published 30 Jun 2010
(C) 2010 OSA

2.7 Statistical analysis

Data were analyzed using GraphPad Prism 5.0 (GraphPad Software, La Jolla, CA) and presented as mean ± SD. Comparison of LSI with LDV was done by linear regression analysis and Pearson's correlation analysis. Comparative analysis of tissue perfusion measured with LSI at different time points was performed using ANOVA. Differences were considered statistically significant at $p<0.05$.

3. Results

3.1 Complete renal I/R experiments

RBF, MAP, LSI, and LDV measurements during the complete renal I/R experiments, with ischemic episodes of 1 min (n = 5), 10 min (n = 5), and 45 min (n = 5), are presented in Fig. 1. Panels A-C of Fig. 1 depict the results for the 1 min I/R experiment and panel D depicts the reperfusion phase of the 1, 10, and 45 min I/R experiments.

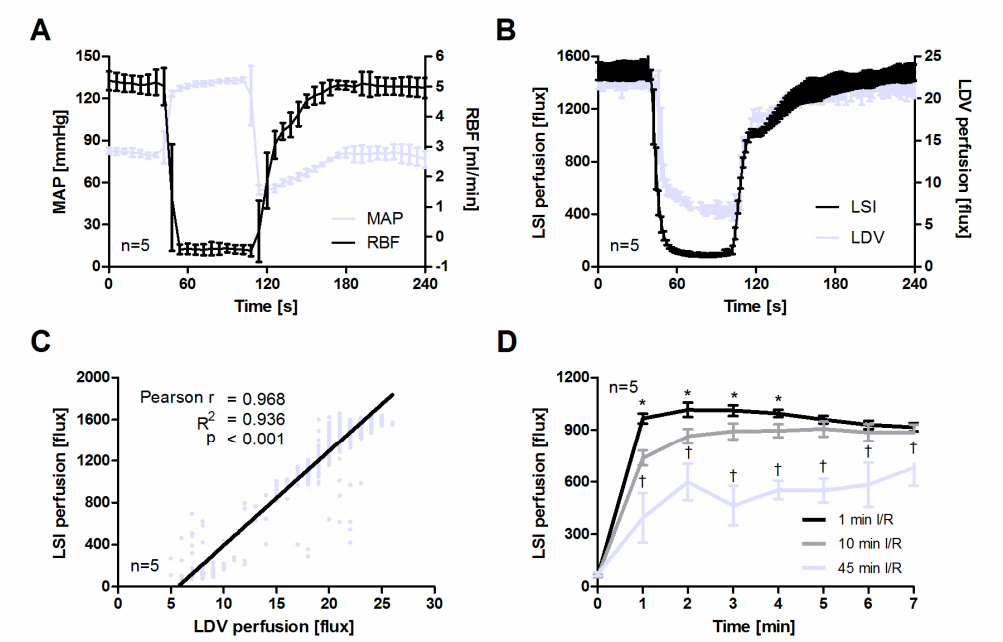

Fig. 1. A: Mean arterial pressure (MAP) and renal blood flow (RBF) during the 1 min ischemia/reperfusion (I/R) experiments. B: Laser speckle imaging (LSI) and laser Doppler velocimetry (LDV) measurements during the 1 min I/R experiments. C: Correlation and linear regression analysis of the LSI and LDV measurements during the 1 min I/R experiments. D: LSI perfusion during the reperfusion phase of the 1, 10, and 45 min I/R experiments. *$p<0.05$ for 1 min I/R versus 10 min I/R and $^{\dagger}p<0.05$ for 45 min I/R versus 1 min I/R and 10 min I/R.

Suprarenal aortic occlusion led to stopped RBF and microvascular perfusion (measured using LSI and LDV) and an increased MAP (Figs. 1A and B). In the 1 min I/R experiments, LSI was performed in combination with LDV and the techniques exhibited a strong correlation (Pearson r = 0.968) and linear relation ($R^2 = 0.936$, $p<0.001$) (Fig. 1C). However, the 'background flux' (i.e., the measured flux at zero perfusion) was approximately 25% higher with LDV compared to with LSI. Figure 1D shows that LSI is able to detect differences in reperfusion dynamics following different durations of ischemia. Furthermore, LSI evinced that renal cortical microvascular reperfusion is depressed following 45 min of ischemia early in the reperfusion phase.

#125295 - $15.00 USD Received 11 Mar 2010; revised 6 May 2010; accepted 12 May 2010; published 30 Jun 2010
(C) 2010 OSA

3.2 Heterogeneous I/R experiment

To demonstrate the ability of LSI to image highly heterogeneous microvascular perfusion in the kidney, air bubble-enriched isotonic saline was infused, randomly obstructing microcirculatory branches. A typical experiment is shown in Fig. 2. Infusion of air bubble-enriched isotonic saline first led to complete obstruction of the renal cortical artery (Fig. 2B, 7 s post-infusion) after which the bubbles gradually dissolved (maximal heterogeneity; Fig. 2C, 14 s post-infusion) until normal renal cortical perfusion was restored (Fig. 2D, 21 s post-infusion). As the kidney is somewhat spherical rather than flat, one region on the kidney surface has the exact angle with respect to the light source and the CCD camera such that it directly reflects the illumination light onto the camera. In this region, therefore, the camera is overexposed and the LSI perfusion calculation fails as shown in Fig. 2.

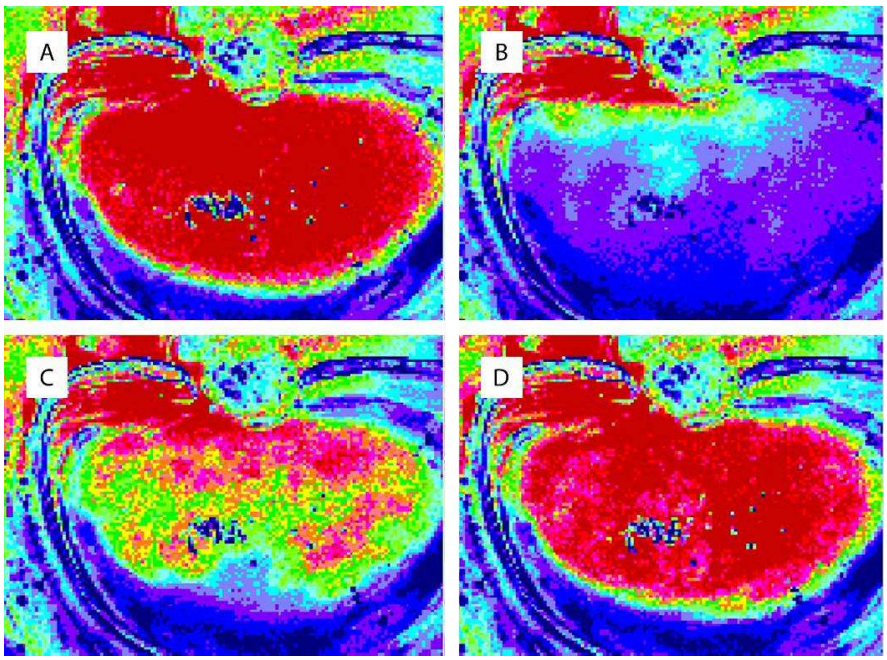

Fig. 2. Laser speckle imaging (LSI) perfusion maps before (A) and after (B-D) infusion of air bubble-enriched isotonic saline. The air bubbles first led to complete obstruction of the renal cortical artery (B, 7 s post-infusion) after which the bubbles gradually dissolved (C, 14 s post-infusion) until normal renal cortical perfusion was restored (D, 21 s post-infusion).

Figure 3A shows that the average native LSI perfusion heterogeneity (i.e., the SD of the Gaussian fit of the LSI perfusion histogram) in the kidney was approximately 190 flux. The maximum perfusion heterogeneity following infusion of the air bubble-enriched isotonic saline was approximately 60 flux (i.e., ~30%) higher than the native perfusion heterogeneity as shown in Fig. 3B.

#125295 - $15.00 USD Received 11 Mar 2010; revised 6 May 2010; accepted 12 May 2010; published 30 Jun 2010
(C) 2010 OSA

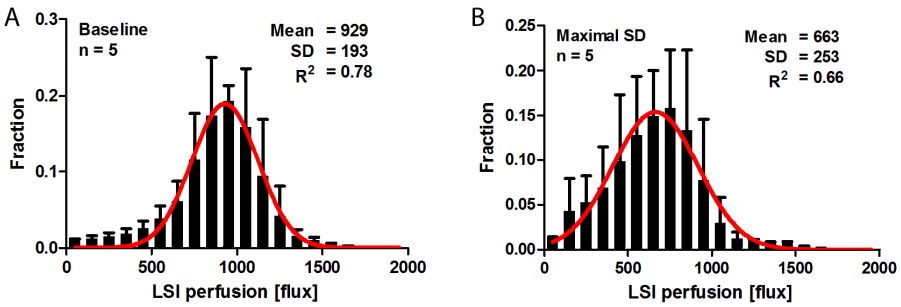

Fig. 3. Laser speckle imaging (LSI) perfusion histograms before (A) and after (B) infusion of air bubble-enriched isotonic saline. The histograms were fitted with a Gaussian fit to determine the mean ± SD of the LSI perfusion histograms. The SD of the Gaussian fit of the LSI perfusion histograms was interpreted as a measure of perfusion heterogeneity.

4. Discussion and conclusions

This is the first study to employ LSI for assessing renal cortical microvascular perfusion heterogeneities. We have used two types of LSI image analysis yielding either a single LSI perfusion value for the entire renal cortex or an LSI perfusion histogram, describing the perfusion heterogeneity in the renal cortex. The main findings were that: 1) full-field LSI measurements of renal microvascular perfusion were highly correlated to single-point LDV measurements; 2) LSI is able to detect differences in reperfusion dynamics following different durations of ischemia; and 3) renal microvascular perfusion heterogeneities can be quantitatively assessed by recovering LSI perfusion histograms.

Although both LSI and LDV are based on optical scattering by flowing cells and express the measured 'velocity' in units of flux, the flux-values provided by these techniques have a different physical and technical background as described elsewhere [18]. When comparing LSI and LDV during I/R (Fig. 1B), we found that LDV has a higher 'background flux', which is probably a technological rather than a physical issue as the LDV device employed here is a fiber-based system that possibly introduces additional background noise due to internal reflections in the fiber. The LSI device, being a non-contact system, does not have this problem. Overall, however, LSI and LDV showed good agreement during the I/R experiments. Several other studies have shown good agreement between LSI and LDV measurements [23–25]. Dunn et al. [23] demonstrated that LSI and LDV measurements of cerebral blood flow were linearly related (R^2 = 0.98) during focal ischemia and cortical spreading depression in rats. Moreover, Forrester et al. [24] showed that LSI and LDV measurements respond similarly to perfusion alterations in the human skin and rabbit muscle during I/R and thermal stress. In addition, Stewart et al. [25] have shown that a linear relation (R^2 = 0.86) between LSI and LDV measurements also exists in skin burn scars. However, none of these studies were performed on the kidney in which microvascular perfusion heterogeneities are considered a major complication underlying AKI. The present study therefore serves as a frame of reference for future investigations focusing on renal microvascular perfusion heterogeneities under (patho)physiological conditions.

Furthermore, two types of image analysis were used, illustrating the wide range of experimental (and clinical) LSI applications for the detection of microvascular perfusion alterations. Using LSI we were able to detect differences in reperfusion dynamics following different durations of ischemia and it could be shown that renal cortical microvascular reperfusion is depressed following 45 min of ischemia early in the reperfusion phase. LSI can furthermore be employed, for instance, for measuring microvascular perfusion in vital (e.g., kidney) and non-vital (e.g., gut) organs simultaneously to monitor blood flow redistribution during shock and resuscitation. Additionally, the generation of LSI perfusion histograms provides a quantitative method for scoring microvascular perfusion heterogeneities in time.

#125295 - $15.00 USD Received 11 Mar 2010; revised 6 May 2010; accepted 12 May 2010; published 30 Jun 2010
(C) 2010 OSA

In previous studies investigating renal oxygenation distributions in a rat model of endotoxemia [27,28], the width of the oxygenation histograms was considered a measure of oxygenation heterogeneities and was shown to be related to renal dysfunction. Here, we applied a Gaussian function (providing a mean ± SD) to characterize the shape, and thereby the width (reflected by the SD), of the LSI perfusion distributions. Although in this model of heterogeneous I/R, the LSI perfusion distributions were well-described by a mean- and SD-value. In other scenarios, however, a different descriptor, such as a medium and interquartile range, might be used.

Alternative techniques for imaging organ perfusion heterogeneities are scanning LDV [12], thermography or infrared imaging [13,26], and NADH autofluorescence imaging [12,15,16]. Scanning LDV is a relatively slow technique (typically 10-60 s/image) and therefore very sensitive to movement artifacts and not capable of measuring rapid perfusion changes under I/R conditions [12]. Thermography, in contrast, is capable of generating images of tissue perfusion at a high frame rate [26]. However, thermography is based on changes in tissue temperature following changes in tissue perfusion and is therefore integrative in both the time- and space-domain. Due to the thermal capacity of the tissue, rapid changes in tissue perfusion do not immediately induce rapid changes in tissue temperature and, furthermore, thermal diffusion limits the spatial resolution of the technique. Moreover, the temperature distribution visualized by the infrared camera is determined by a number of factors, including convection, heat generation by metabolic processes, and heat dissipation at the organ surface, and hence does not solely reflect organ perfusion [13]. Similar arguments hold for NADH autofluorescence imaging, where the NADH level depends on both oxygen delivery by microvascular blood flow and oxygen utilization by metabolic processes [11,14,15]. An increase of the NADH level indicates that the balance of oxygen delivery and utilization is disturbed and that microvascular perfusion is insufficient in oxygenating the organ. NADH autofluorescence imaging is therefore able to identify hypoxic tissue areas, but does not directly reflect tissue microvascular perfusion. Hence, both thermography and NADH autofluorescence imaging are indirect measures of renal microvascular perfusion, while the LSI signal is directly and linearly related to microvascular red blood cell velocity [18–21]. Furthermore, the 25 Hz LSI image acquisition rate allows the detection of rapid changes (Fig. 1B) and spatial variations (Fig. 2) in perfusion in the entire field of view.

LSI has, however, some technical limitations. First, as the technique is based integration of fluctuations in the laser speckle pattern, it is sensitive to movement artifacts. However, the sensitivity of LSI to movement artifacts is much lower compared to that of scanning LDV due to the much shorter image acquisition time of LSI (i.e., ~4 ms for LSI versus 10-60 s for scanning LDV). Nevertheless, movement artifacts, for example caused by animal respiration, are an important issue possibly leading to misinterpretation of (falsely) measured LSI perfusion. In the present study, we prevented kidney movement by stabilizing it in a kidney cup. Second, LSI equipped with a 780-nm laser diode for illumination has an imaging depth of approximately 300-600 μm and is therefore limited to the organ surface [12]. In case of renal imaging, this is not per se a shortcoming of the technique, as renal microcirculatory heterogeneities have been shown to be more prominent in the renal cortex as opposed to the renal medulla [4,5,27,28]. Hence, focusing on the renal cortex rather than the cortex and medulla might prove to be more sensitive to the pathophysiological conditions underlying AKI.

In conclusion, in the present study we have evaluated the use of LSI for mapping renal cortical microvascular perfusion heterogeneities. We found that LSI and LDV measurements were in good agreement and that LSI is able to detect differences in reperfusion dynamics following different durations of ischemia. We have furthermore shown that LSI enables simultaneous assessment of renal microvascular perfusion in different regions of the renal cortex at high temporal and spatial resolution and that the generation of LSI perfusion histograms provides a quantitative method for scoring renal microvascular perfusion heterogeneity in time.

#125295 - $15.00 USD Received 11 Mar 2010; revised 6 May 2010; accepted 12 May 2010; published 30 Jun 2010
(C) 2010 OSA